PCCP

Accepted Manuscript

ROYAL SOCIETY OF CHEMISTRY

www.rsc.org/pccp

Negative ion states of 5-bromouracil and 5-iodouracil

F. Kossoski[1] and M. T. do N. Varella[1]

Instituto de Física, Universidade de São Paulo, Caixa Postal 66318, 05314-970, São Paulo, São Paulo, Brazil

The valence anion states of the potential radiosensitisers 5-bromouracil and 5-iodouracil were investigated through elastic scattering calculations. These compounds have rich spectra of negative ion states that trigger off different mechanisms for dissociative electron attachment. For each molecule, we obtained a bound π^* anion, two π^* shape resonances and a low lying σ^* anion state, in addition to a dipole-bound state (the latter was obtained from bound-state techniques). The σ^* anion, formed by electron attachment to an anti-bonding carbon-halogen orbital, was found to have resonant character in 5-bromouracil, and bound-state character in 5-iodouracil. The present calculations place the σ^*_{CBr} resonance around 0.7 eV, considerably below the energy inferred from the electron transmission data (1.3 eV). The signature of this anion state, not evident in the measurements, would be obscured by the large background arising from the dipolar interaction, not by the strong signature of the π_2^*, as presumed. Our results support the π_2^* resonance as a precursor state to dissociative electron attachment around 1.5 eV in both 5-bromouracil and 5-iodouracil, while the interplay among π_1^*, σ^* and dipole-bound states would be expected close to 0 eV. We also discuss the suppression of the hydrogen elimination channels in these species.

PACS numbers: 34.80.Bm, 34.80.Gs

I. INTRODUCTION

Large amounts of low-energy electrons (LEEs) ($0 - 30\,\mathrm{eV}$) are generated along the track of ionising radiation in the biological medium. Prior to solvation, these ballistic electrons can be captured into unoccupied molecular orbitals, thus giving rise to transient negative ions, or resonances. If the resonant state lives for long enough, the geometrical relaxation induced by electron capture may give rise to bond cleavages, and this process is referred to as dissociative electron attachment (DEA). It is now well established that biomolecules often undergo DEA, which is the underlying mechanism for the electron-induced single and double strand breaks in DNA[1] that may damage the genetic code and ultimately result in cell death. While the attack of LEEs to healthy cells is an unwanted consequence of ionising radiation, it would become desirable in case the detrimental effects were, as much as possible, restricted to cancer cells. The damage to tumour cells can actually be favoured by incorporating radiosensitising drugs to the gene sequence through chemotherapy. The direct relation between large DEA cross sections and enhanced radiosensitivity[2] indicates that the latter could arise from efficient DEA processes at the molecular level. It is therefore important to better understand the fundamental interactions between electrons and molecules with potential radiosensitising activity.

Halopyrimide molecules, in particular the halouracils, are well known radiosensitisers[3,4], and their capability of enhancing the LEE damage to nucleosides and trinucleotides was demonstrated in recent experiments[5,6]. In particular, 5-bromouracil (BrU) and 5-iodouracil (IU) can be incorporated into DNA, replacing thymine units, and enhance free radical damage[4]. They also have very large DEA cross sections[7] and might be the most efficient radiosensitisers among the 5-halouracils. In spite of the interest on LEE interactions with halouracils, and their relevance to radiation biology, the available information on the transient anion spectra of BrU and IU is sketchy at best. To our knowledge, no studies on the transient anion states of IU have been reported, while the electron transmission (ET) spectrum of BrU was measured by Scheer *et al.*[8]. The latter provided invaluable information on the shape resonances of this species, but a question on the energy of the lowest σ^* anion was left open.

The knowledge on the resonance spectra is important *per se* and also useful to help the interpretation of the available DEA data[2,7,9–11] , since the formation resonant states

trigger off the dissociation dynamics. In this work, we survey the shape resonance spectra of BrU and IU, as obtained from integral cross sections (ICSs) for elastic electron scattering, computed with the Schwinger multichannel method. We also study the dipole bound states (DBS's), not considered in previous studies, as well as the valence bound states (the latter have been addressed by Wetmore *et al.*[12] and Li *et al.*[13], although only for BrU). We hope the present results can provide a reasonably complete picture of the anion state spectra of BrU and IU below the electronic excitation regime (core-excited resonances)

This paper is organised as follows. The computational methods and procedures are outlined in Sec. II, while in Secs. III and IV we present and discuss our results. In Sec. V we summarise our main findings and conclusions.

II. COMPUTATIONAL PROCEDURES

The fixed-nuclei scattering calculations were performed at the equilibrium geometries of the electronic ground states of BrU and IU. The geometry optimisations were carried out with Density Function Theory (DFT) and the hybrid B3LYP functional. For BrU we employed the 6-31++G(2d,1p) basis set, while for IU the basis set described in Refs.[14,15], which has 6-311G(d,p) quality. Once the optimal geometries were obtained, the target ground state and the scattering calculations were carried out replacing the nuclei and core electrons of the heavier atoms (all but hydrogen) by the norm-conserving pseudopotentials of Bachelet, Hamann and Schlüter (BHS)[16]. This procedure significantly reduces the computational effort, in view of the large number of core electrons in the bromine and iodine atoms, and also incorporates scalar relativistic effects (spin-orbit couplings were not accounted for). The electronic ground state was described at the restricted Hartree-Fock level employing Cartesian Gaussian basis sets generated according to Bettega *et al.*[17], which are suitable for use with the BHS pseudopotentials. We employed a $6s5p2d$ basis set for the bromine and iodine atoms and a $5s5p2d$ basis set for the carbon, nitrogen and oxygen atoms, whose exponents are shown in Tab. I. For the hydrogen atoms we employed the $3s$ basis set of Dunning, Jr.[18]. The Gamess package[19] was employed for the geometry optimization and the ground state description.

The elastic ICSs were computed with the Schwinger multichannel method[20], using both the BHS pseudopotentials[21] and parallel processing[22]. The collision simulations would be

extremely time-consuming otherwise. Here we restrict the discussion of the method to the important aspects concerning the present application. The working expression for the scattering amplitude is given by

$$f(\vec{k}_f, \vec{k}_i) = -\frac{1}{2\pi} \sum_{m,n} \langle S_{\vec{k}_f} | V | \chi_m \rangle \left(d^{-1} \right)_{mn} \langle \chi_n | V | S_{\vec{k}_i} \rangle \, , \tag{1}$$

where

$$d_{mn} = \langle \chi_m | \, A^{(+)} \, | \chi_n \rangle \tag{2}$$

and

$$A^{(+)} = \frac{\hat{H}}{N+1} - \frac{(\hat{H}P + P\hat{H})}{2} + \frac{(VP + PV)}{2} - VG_P^{(+)}V. \tag{3}$$

In the above equations $|S_{\vec{k}}\rangle$ is an eigenstate of the unperturbed Hamiltonian H_0, given by the product of a plane wave with momentum $\vec{k}$ and the target ground state; V is the interaction potential between the target molecule and the incoming electron; $\hat{H} = E - H$ is the collision energy minus the full Hamiltonian $H = H_0 + V$; N is the number of electrons in the target; P is a projection operator onto the open electronic states of the target; and $G_P^{(+)}$ is the free particle Green's function projected on the P space.

Since the present application is restricted to elastic scattering, the open-channel space only comprises the target ground state, $P = |\Phi_0\rangle\langle\Phi_0|$. The scattering wave function is expanded in a set of configuration state functions (CSF's), $\{|\chi_m\rangle\}$, given by spin-adapted $(N+1)$-electron Slater determinants. These configurations are built as products of target states and single-particle functions (scattering orbitals). In the lower level static-exchange (SE) approximation, the CSFs are given by $|\chi_j\rangle = A[|\Phi_0\rangle \otimes |\varphi_j\rangle]$, where $|\Phi_0\rangle$ is the target ground state, $|\varphi_j\rangle$ is the scattering orbital and A is the antisymmetriser. In the more accurate static-exchange plus polarisation (SEP) approximation, the CSF space comprises configurations generated as $|\chi_{ij}\rangle = A[|\Phi_i\rangle \otimes |\varphi_j\rangle]$, where $|\Phi_i\rangle$ is an excited virtual target state obtained by promoting a single electron from an occupied (hole) to an unoccupied (particle) orbital. Modified virtual orbitals (MVOs)[23] generated from cationic Fock operators with charge +12 were used to represent both the particle and scattering orbitals.

The ICSs were computed separately for the A' and A'' components of the C_s point group (both molecules have planar ground states). For both symmetries, the CSF space was

generated according to the energy criterion[24] $\varepsilon_{scat} + \varepsilon_{part} - \varepsilon_{hole} < \Delta$, where ε_{scat}, ε_{part} and ε_{hole} are the energies of the scattering, particle and hole orbitals, respectively, and Δ is an energy threshold. Since the number of valence electrons in both molecules is the same, a balanced description of the polarisation effects requires CSF spaces of similar size. To achieve this balance, we employed different energy cutoff values for each system, namely $\Delta = -3.40$ and $\Delta = -3.30$ Hartree for BrU and IU, respectively. For both targets, we allowed for singlet- and triplet-coupled target excitations, although only retaining doublets in the CSF space. We obtained a total of 18903 configurations for BrU (9653 in the A' and 9250 in the A'' symmetry components) and 18586 for IU (9488 in A' and 9098 in A''). The SEP approximation provides more accurate results that will be compared to the elastic scattering data. We also report the less accurate SE calculations, known to overestimate the anion state energies, because the difference between SE and SEP results indicates the contribution from correlation-polarization effects to the latter.

While the present approach employs finite-range trial scattering wave functions (built on Gaussian orbitals), it can accurately describe the low angular momentum components where the resonance signatures are found. We did not employ any procedure to account for the long-range dipole potential contribution to the higher partial waves. This contribution would significantly impact only the background cross section and obscure the resonance states[25,27]. Since our main purpose is obtaining the transient anion spectra, we report symmetry-resolved cross sections without correcting the higher partial waves to highlight the resonance signatures (even though the cross section magnitudes are underestimated). As stated above, the elastic ICSs are obtained in the fixed-nuclei approximation and including only the target ground state in the open-channel operator P in eqn (3). We also average over the initial target orientations (in consistency with the gas-phase experiments) and integrate over the outgoing scattering angles. The assignment of resonance energies and widths are obtained from least-squares fits of Breit-Wigner profiles, $\delta_{\rm sum}(E) = \delta_{\rm bg}(E) + \delta_{\rm res}(E)$, to the calculated eigenphase sums ($\delta_{\rm sum}$). We employ the usual parametrization to the resonant component, $\delta_{\rm res}(E) = -\tan[\Gamma/2(E - E_{\rm res})]$, where $E_{\rm res}$ and Γ are the resonance position and width, respectively, and second-degree polynomials to model the background component ($\delta_{\rm bg}$).

The scattering wave functions described above would be expected to account for the resonant and valence bound anion states. To obtain the DBS's, wherein the additional electron

occupies a very diffuse orbital on the positive end of the target molecule, we employed the alternative procedure suggested by Skurski *et al.*[28]. The aug-cc-pVDZ basis set was augmented with a set of $6s6p$ diffuse functions placed on the hydrogen at the 1 site (see Fig. 4), lying on the positive pole of the permanent dipole moment. The extra set was generated in an even-tempered fashion, starting from the most diffuse exponent of hydrogen in the aug-cc-pVDZ set and successively dividing the exponents by 4. For the iodine atom we employed the aug-cc-pVDZ-PP basis set and the pseudopotentials described in Ref.[29]. With these augmented sets in hand, the neutral ground states were optimised at the Møller-Plesset second-order perturbation theory (MP2). Single-point calculations were then performed for the neutral and anion states, with the MP2 and coupled-cluster methods, accounting for single, double and perturbative triple excitations in the latter case (CCSD(T)). The computation of DBS's was performed with the Gaussian09[30] software, without accounting for vibrational zero-point corrections.

Finally, we also employed Gaussian09 to estimate reaction thresholds for uracil, 5-fluorouracil (FU), 5-chlorouracil (ClU) and BrU, computed with the G4(MP2) method. However, since the standard basis sets employed in this composite method are not available for the iodine atom, it cannot be applied to IU. We did not attempt to modify the G4(MP2) approach to account for the iodine atom because the IU dissociation thresholds would not significantly change the discussion on the dissociation mechanisms (see Sec. IV).

III. RESULTS

The elastic ICSs obtained for BrU are shown in Fig. 1. At the SE approximation three π^* resonances are found, at 1.74, 3.92 and 7.4 eV, hereafter called π_1^*, π_2^* and π_3^*. Inclusion of polarisation effects shifts these states to lower energies, namely 1.50 and 4.45 eV for the higher lying π_2^* and π_3^* states, respectively. The calculated resonance positions compare favourably with the experimental values of 1.3 and 3.6 eV, obtained from ET measurements by Scheer *et al.*[8] The larger discrepancy for the π_3^* resonance is expected, and arises from the mixed shape and core-excited character[31,32]. It would be remedied with the inclusion of triplet-coupled target states in the open channel space (these are neglected in the single-channel model employed in this work). In the SEP approximation, the π_1^* state is absent from the computed ICS, as it becomes a bound valence state. The diagonalisation of the

Hamiltonian in the CSF basis indicates a binding energy of −0.30 eV (bound and resonance states are indicated with negative and positive energies, respectively), somewhat larger, in absolute value, than those previously reported by Wetmore *et al.*[12] (−0.17 eV) and Li *et al.*[13] (−0.11 eV).

Scheer *et al.*[8] pointed out that a σ^*_{CBr} shape resonance, although expected from virtual orbital analysis, was not evident in the ET spectrum. These authors argued that the signature of the σ^*_{CBr} anion could have been obscured by the more intense signal of the π^*_2 resonance, i.e., they inferred both negative ions would lie very close to each other. The superposition of these anion state signatures can be avoided by the symmetry decomposition of the computed cross sections. In fact, a σ^*_{CBr} resonance around 3.7 eV is evident in the SE A' component (Fig. 1). Even though the signature of this anion state is not clear in the SEP calculation, no valence bound state was obtained from the diagonalisation of the scattering Hamiltonian in the CSF basis (in contrast to the π^*_1 anion state in the A'' component, as discussed above). We therefore believe a low lying σ^*_{CBr} resonance actually exists, as clearly pointed out by the SE result, even though its signature in the SEP calculation is hidden by the large background arising from the dipolar interaction, despite the neglect of the corrections to the higher partial waves in the present calculations (these would give rise to an even larger background, see Sec. II). To make this point more clear, we have carried out additional calculations with intermediate configuration spaces between the SE approximation (no polarization) and the SEP result shown in Fig. 1 (comprising 9563 CSFs in the A' subspace, see Sec. II), which we consider our most reliable calculation. The results are shown in the upper panel of Fig. 2, where the description of polarization is gradually improved with the energy cutoffs $\Delta = -4.2, -3.8, -3.6, -3.5$ hartree, which give rise to 1017, 3344, 5820 and 7531 configurations, respectively. As the σ^*_{CBr} resonance gradually shifts to lower energies, as expected, its signature becomes less clear and barely noticeable below 1 eV, where the dipolar background is very large (as indicated by the slope of the calculated cross sections). The position and energy of the σ^*_{CBr} anion, obtained from the least-squares fits to the eigenphase sums, are plotted against the number of CSFs in the lower panel of Fig. 2. From the 9563-CSF calculation, we estimate the resonance position and width around 0.73 eV and 0.60 eV, respectively. The position estimate is supported by the diagonalisation of the scattering Hamiltonian represented in the CSF basis, which points out a pseudo-eigenstate with σ^*_{CBr} character around 0.61 eV. We therefore believe the σ^*_{CBr}

anion state would not be obscured by the π_2^* signal in the ET spectrum (the calculations indicate a 0.8eV spacing between them), but rather from the large background, the low energy of the σ^*_{CBr} resonance, and its significant 0.60 eV width that overlaps the threshold. Finally, two structures are discernible in the A' symmetry, around 6.5 and 9 eV, possibly originating from the occupation of higher lying σ^* orbitals. However, since we do not include any open excited states in the present calculations, we refrain from discussing these higher lying structures.

The computed elastic ICS components of IU are shown in Fig. 3. Once more, the SE approximation indicates three distinct peaks in the A'' symmetry, at 1.78, 3.86 and 7.2 eV, which are signatures of π^* anion states. The A' component displays a structure at 2.1 eV, arising from electron attachment to a σ^*_{CI} orbital. In the improved SEP results, the π_1^* anion becomes a bound state (-0.35 eV), while the π_2^* and π_3^* shape resonances appear at 1.54 and 4.34 eV, respectively. In contrast to BrU, the diagonalisation of the scattering Hamiltonian in the A' space indicates a bound σ^*_{CI} state at -0.10 eV, lying vertically below the neutral ground state. The presence of a bound σ^* state would distinguish IU from the other 5-halouracils, all having σ^*_{CX} resonances[25,26], where X denotes the halogen atom. In view of the small calculated binding energy, however, we cannot rule out the existence of a very low lying resonance ($\gtrsim 0$ eV). Finally, higher lying structures are also found in the A' ICS, around 5.8 and 9 eV.

To gain further insight into the resonance characters, we obtained the virtual orbitals shown in Fig. 4 using compact basis sets. The virtual orbital energies (VOEs) were also used to estimate vertical attachment energies (VAE's), as suggested by Staley and Strnad[33]. According to their procedure, the target geometries were optimised at the MP2/6-31G(d) level, and the canonical HF virtual orbitals were computed with the same geometries and basis sets. The attachment energies to π^* orbitals were then calculated from the scaling relation (in units of eV) VAE = 0.64795×VOE−1.4298. For BrU, the empirical scaling predicts π^* states at 0.03, 1.39 and 3.84 eV, while those of IU would be found at 0.01, 1.37 and 3.65 eV. In general, the estimates are close to the present scattering results, although the VOE scaling indicates resonant π_1^* states, with nearly zero energies, for both molecules (in disagreement with the ET data for BrU[8]). The π_2^* resonances of BrU and IU are predicted to lie close to each other (at 1.39 and 1.37 eV, respectively), also in agreement with the present calculations (1.50 eV in BrU and 1.54 eV in IU). We also applied the alternative relation

(in units of eV) VAE = (VOE −3.23)/0.99, proposed by Pshenichnyuk *et al.*[34] to estimate the VAE's to σ^*_{CBr} orbitals in bromoalkanes, to BrU. The attachment energy of 0.72 eV also agrees well with our prediction based on the eigenphase sums.

For BrU, we obtained the DBS energies of −42 and −71 meV from the MP2 and CCSD(T) calculations, respectively. For IU, the calculated energies were −39 meV (MP2) and −75 meV (CCSD(T)). Since there are, to our knowledge, no available experimental data on the dipole binding energies for these molecules, we employed the same methodologies to uracil, having a DBS around −90 meV[35,36]. The calculated results are close to those of the halogenated forms, −44 meV (MP2) and −65 meV (CCSD(T)), suggesting that BrU and IU could also have DBS's around −90 eV. The singly occupied molecular orbital of the DBS is also shown in Fig. 4. In this case, however, the orbital was not obtained from the MP2/6-31G(d) method used for the valence orbitals, but from an unrestricted Hartree-Fock calculation with the diffuse basis set described in Sec. II.

In Tab. II the positions and widths of the anion states of BrU and IU are presented, comprising the present scattering calculations, previous bound-state calculations[12,13], and ET measurements[8]. The π^* orbitals for the series of 5-halouracils are very similar to those of BrU, shown in Fig. 4. According to our scattering results and the ET data[8], the π_1^* state shifts to lower energies as the halogen atomic number increases, while the π_2^* and π_3^* resonances do not present a clear stabilisation pattern. In contrast to the relatively small differences in energy among the π^* states, the dissociative σ^* states present a clear trend. According to the present and the previous calculations[25], the signature of this anion state in the ICS of FU is not evident[26]. It then appears around 2.5 eV in the ICS of ClU, shifts down to 0.7 eV in BrU (although obscured by the background) and finally becomes a shallow bound state (−0.1 eV) in IU.

IV. DISCUSSION

The DEA spectra of BrU and IU share several common features[2,7,9–11] below the electronic excitation threshold that can be interpreted from the present results. Our discussion is also based on the zero-temperature dissociation thresholds shown in Tab. III for uracil, FU, ClU and BrU. It is noteworthy that the G4(MP2) method provides thresholds for C–X bond breakings ~ 0.3 eV below previous computations[12,13,38,39], even though the present estimates

for the hydrogen elimination thresholds (N_1 site) are in good agreement with those studies. Since thermal degradation[38] and vibrationally hot bands[8] have been considered to explain the low-energy fragmentation of the halouracils, we have computed the vibrational thermal energies employing the harmonic approximation (sum over uncoupled vibrational modes) and the appropriate Boltzmann distributions for the vibrational frequencies obtained at the DFT/B3LYP/aug-cc-pVTZ level. Apart from the zero-point energy contributions, the halouracils have average vibrational energies around $\sim 0.3\,\mathrm{eV}$ at 450 K, which would lower the dissociation thresholds shown in Tab. III (this temperature faithfully accounts for the experimental conditions[2,7,9–11,38]). Some qualitative understanding of the couplings among the anion states can be gained from virtual orbital analysis (see below), in the light of well known DEA mechanisms (for a review, see Hotop *et al.*[40] and references therein). More specifically, electron attachment into a π^* resonance diabatically coupled to a dissociative σ^* resonance (indirect mechanism[41]) and the formation of a vibrationally excited DBS coupled to a broad σ^* anion state (direct mechanism[42]). A time-consuming detailed investigation into the potential energy surfaces is beyond the scope of this work, as well as accurate simulations of the DEA dynamics that would require sophisticated nonlocal models[40,43] and the inclusion of several vibrational modes to account for the relevant vibronic couplings.

The most intense DEA signals for BrU and IU arise from the elimination of the halide anions X^-, along with significant yields for the complementary $[XU{-}X]^-$ fragments and the XU^- parent anions. The calculated thresholds and thermal excitation energies are compatible with the X^- fragments observed at $\gtrsim 0\,\mathrm{eV}$, at least for BrU (the present threshold estimates would be expected accurate within $\sim 0.1\,\mathrm{eV}$). However, our results cannot explain the onset of the X elimination reaction at similar collision energies, in view of the significantly higher thresholds.

Close to 0 eV, DEA may operate in BrU and IU through the occupation of valence π_1^* or dipole-bound orbitals, which would couple to the dissociative σ^*_{CX} states. In IU, direct dissociation triggered off by formation of the bound σ^*_{CI} state might also play a role (even if this anion state was a very low-lying resonance it would readily become bound in view of the C–I bond stretch arising from the occupation of the antibonding orbital). Both BrU and IU have DEA peaks for X^- and $[XU{-}X]^-$ at 1.3 eV and 1.4 eV, respectively[7], lying close to the presently reported π_2^* anion states ($\approx 1.5\,\mathrm{eV}$, see Tab. II). This matching indicates that electron capture into the π_2^* orbitals induces halogen elimination (through the coupling to

the σ^*_{CX} anions), as previously suggested[10]. Fragments assigned as OCN^- and $[H_2C_3NO]^-$ were detected at 1.7 eV (BrU) and 1.3 eV (IU), indicating that the π^*_2 resonance may give rise to different dissociation pathways. These fragments were also detected at 3.5 eV in BrU and 4 eV in IU[7], so they could correlate to the π^*_3 resonances (as discussed above, the presently reported energies for the π^*_3 anion states, above 4 eV for both systems, are overestimated).

One of the most intriguing aspects of the DEA data for BrU and IU is the absence of hydrogen elimination signals ($[XU–H]^-$ fragments), in contrast to uracil, FU and ClU. At lower energies, the sharp DEA peaks in uracil are believed to arise from the coupling between the DBS and a dissociative σ^*_{NH} resonance[8,37] (see also Hotop *et al.*[40] and Stricklett *et al.*[42]). Accordingly, electron attachment to the DBS (inner part of the anion state potential curve along the N_1–H reaction coordinate) gives rise to vibrational Feshbach resonances (VFRs), and dissociation follows from tunnelling into the outer part of the potential curve (having σ^*_{NH} character). Analysis of the DBS binding energy, dissociation threshold and the vibrational frequency of the ν_{NH} stretch mode suggests that the DEA peaks around 0.7 eV and 1.0 eV in U arise from the $\nu_{NH} = 2, 3$ VFRs.

As mentioned in Sec. III, uracil and halouracils have fairly similar DBS binding energies, suggesting that the inner part of the potential curves (having DBS character) would also be similar. This was indeed confirmed by exploratory studies of the DBS potential along the N_1–H coordinate (not shown here), which pointed out close ν_{NH} frequencies and transition state energies (arising from the DBS/σ^*_{NH} coupling) for FU, ClU and BrU. While the stabilization of the $[XU–H]^-$ anions gives rise to smaller DEA thresholds from FU to BrU, the differences are somewhat small in comparison with the $\hbar\omega \approx 0.45$ eV excitation energy of the ν_{NH} mode (in particular, the ClU and BrU thresholds are very close). As a consequence, at least for BrU the energetics of the anion state potentials along the N_1–H stretch coordinate would not justify the absence of the $[XU–H]^-$ anion at low energies, where VFRs are observed in uracil, FU and ClU. On the other hand, (i) the lowest-lying compact σ^* orbitals (Fig. 4 and Ref.[25]) suggest $\sigma^*_{N_1H}/\sigma^*_{CX}$ couplings, with increasing probabilities on the C–X bond from FU to IU (IU orbitals not shown in Fig. 4); (ii) Tab. III indicates significantly decreasing thresholds for X^- elimination from FU to BrU (in particular, the X^- threshold is significantly lower than the H elimination counterpart in BrU, unlike FU and ClU); (iii) thermal excitation would be expected more effective for C–X stretch as the halogen mass increases (in contrast to the high-frequency ν_{NH} mode). With respect to the last point, the calculated vibrational

spectra of ClU and BrU are fairly similar. The lowest-energy normal mode with significant C–X stretch character in both systems (ν_5) has a higher frequency in ClU (0.045 eV) than in BrU (0.035 eV) and a larger C–X stretch component in the latter. As a result, the mean occupations at 450K ($k_BT = 39$ meV) are estimated as $\bar{\nu}_5 = 0.46$ (ClU) and $\bar{\nu}_5 = 0.68$ (BrU). Assuming a competition between hydrogen and halogen elimination through the coupled states, the aspects (i) to (iii) above would increasingly favour the latter mechanism from FU to BrU, in consistency with the observed DEA signals at low energies ($\lesssim 1$ eV) along the series: $[FU–H]^-$ and $[FU–HF]^-$ for FU[9]; $[ClU–H]^-$, $[ClU–HCl]^-$, and $Cl^-/[ClU–Cl]^-$ for ClU[9,38]; while only $X^-/[XU–X]^-$[7,9,11] for BrU and IU.

Finally, the hydrogen signal observed around ~ 1.5 eV in uracil and the lighter halouracils[9,38], is also completely absent in BrU and IU[7,9,11]. At this energy the hydrogen atom is released from site 3 (see Fig. 4), since the mechanism involves the coupling of the π_2^* resonance with a $\sigma^*_{N_3H}$ anion state[44]. The inspection of the virtual orbitals obtained from compact basis sets indicates that both the π_2^* orbital and the LUMO+2, having $\sigma^*_{N_3H}$ character (not shown here), are similar for all halouracils, thus suggesting the $\pi_2^*/\sigma^*_{N_3H}$ coupling would not change significantly. In addition to the aspects (i) to (iii) outlined above, which could also help to suppress the hydrogen elimination from the N_3 site, for BrU and IU we observe a significant $\sigma^*_{CX}/\sigma^*_{N_3H}$ mixing (in the virtual orbitals) as the N_3–H bond is stretched, which could favour X^- elimination over hydrogen elimination.

V. SUMMARY

We have reported integral cross sections for elastic electron scattering from 5-bromouracil and 5-iodouracil. The results indicate three π^* anion states in both molecules. The bound π_1^* state could be involved in mechanisms of DEA around $\gtrsim 0$ eV, while the π_2^* resonance should trigger off the halogen elimination around 1.4 eV. BrU also has σ^*_{CBr} shape resonance around 0.7 eV (significantly below the 2.5 eV σ^*_{CCl} resonance reported for ClU[25]) whose signature in the ET spectrum would be obscured by the large background arising from the dipole potential. In IU, the σ^*_{CI} anion is obtained as a valence bound state in the present computational model, even though we cannot rule out the possibility of a very low-lying resonance in view of the small binding energy (-0.1 eV). We also investigated the DBSs in BrU and IU, which could also play a role in the DEA mechanisms at lower energies. These

bound states were found to have similar character and binding energies as the DBS of uracil.

This study concludes our investigation on the anion spectra of the 5-halouracils. While the π^*-state energies do not change significantly along the series, the σ^*_{CX} anions are strongly stabilized from FU to IU. Although the present fixed-nuclei calculations cannot fully elucidate the DEA mechanisms, the computed anion states, vibrational analysis and the virtual orbital analysis are consistent with the stronger X^- elimination signals for the heavier uracils (also with the high DEA cross section magnitudes) and the suppression of the hydrogen elimination channels in these systems.

The presently reported results are consistent with the rich DEA spectra of BrU and IU, corroborating their ability for form several anion states that undergo different dissociation pathways. A better understanding of these fundamental processes and their efficiency in biological environments are crucial steps to fully explore their potential as radiosensitizers.

ACKNOWLEDGMENTS

F. K. and M. T. do N. V. acknowledge financial support from Fundação de Amparo à Pesquisa do Estado de São Paulo (FAPESP). M. T. do N. V. acknowledge support from Conselho Nacional de Desenvolvimento Científico e Tecnológico (CNPq). This work employed computational resources from LCCA-USP and CENAPAD-SP.

REFERENCES

[1]B. Boudaïffa, P. Cloutier, D. Hunting, M. A. Huels, and L. Sanche, Science **287**, 1658 (2000).

[2]H. Abdoul-Carime, M. A. Huels, E. Illernberger, and L. Sanche, J. Am. Chem. Soc. **123**, 5354 (2001).

[3]S. Zamenhof, R. Degiovanni, and S. Greer, Nature **181**, 827 (1958).

[4]P. Wardman, Clin. Oncol. **19**, 397 (2007).

[5]C.-R. Wang and Q.-B. Lu, J. Am. Chem. Soc. **132**, 14710 (2010).

[6]Z. Li, P. Cloutier, L. Sanche, and J. R. Wagner, J. Phys. Chem B **115**, 13668 (2011).

[7]H. Abdoul-Carime, M. A. Huels, E. Illenberger, and L. Sanche, Int. J. Mass Spec. **228**, 703 (2003).

[8]A. Scheer, K. Aflatooni, G. Gallup, and P. Burrow, Phys. Rev. Lett. **92**, 068102 (2004).

[9]R. Abouaf and H. Dunet, Eur. Phys. J. D **35**, 405 (2005).

[10]H. Abdoul-Carime, M. A. Huels, F. Brüning, E. Illenberger, and L. Sanche, J. Chem. Phys. **113**, 2517 (2000).

[11]R. Abouaf, J. Pommier, and H. Dunet, Int. J. Mass Spec. **226**, 397 (2003).

[12]S. D. Wetmore, R. J. Boyd, and L. A. Eriksson, Chem. Phys. Lett. **343**, 151 (2001).

[13]X. Li, L. Sanche, and M. D. Sevilla, J. Phys. Chem. A **106**, 11248 (2002).

[14]R. Krishnan, J. S. Binkley, R. Seeger, J. A. Pople, J. Chem. Phys. **72**, 650 (1980).

[15]M. N. Glukhovstev, A. Pross, M. P. McGrath, L. Radom, J. Chem. Phys. **103**, 1878 (1995).

[16]G. B. Bachelet, D. R. Hamann, and M. Schlüter, Phys. Rev. B **26**, 4199 (1982).

[17]M. H. F. Bettega, A. P. P. Natalense, M. A. P. Lima, and L. G. Ferreira, Int. J. Quantum Chem. **60**, 821 (1996).

[18]T. H. Dunning, Jr., J. Chem. Phys. **53**, 2823 (1970).

[19]M. W. Schmidt, K. K. Baldridge, J. A. Boatz, S. T. Elbert, M. S. Gordon, J. H. Jensen, S. Koseki, N. Matsunaga, K. A. Nguyen, S. J. Su, T. L. Windus, M. Dupuis, and J. A. Montgomery, J. Comput. Chem. **14**, 1347 (1993).

[20]K. Takatsuka and V. McKoy, Phys. Rev. A **24**, 2473 (1981); **30**, 1734 (1984).

[21]M. H. F. Bettega, L. G. Ferreira, and M. A. P. Lima, Phys. Rev. A **47**, 1111 (1993).

[22]J. S. dos Santos, R. F. da Costa, and M. T. do N. Varella, J. Chem. Phys. **136**, 084307 (2012).

[23]C. W. Bauschlicher, Jr., J. Chem. Phys. **72**, 880 (1980).

[24]F. Kossoski and M. H. F. Bettega, J. Chem. Phys. **138**, 234311 (2013).

[25]F. Kossoski, M. H. F. Bettega, and M. T. do N. Varella, J. Chem. Phys. **140**, 024317 (2014).

[26]The computed cross sections for FU do not indicate a σ^*_{CF} resonance[25]. However, a bound σ^*_{CF} anion appears as the C–F bond is stretched, thus indicating that a broad resonance would exist in the equilibrium geometry of the neutral molecule.

[27]E. M. de Oliveira, R. F. da Costa, S. d'A. Sanchez, A. P. P. Natalense, M. H. F. Bettega, M. A. P. Lima and M. T. do N. Varella, Phys. Chem. Chem. Phys. **15**, 1682 (2013).

[28]P. Skurski, M. Gutowski, and J. Simons, Int. J. Quant. Chem. **80**, 1024 (2000).

[29]K. A. Peterson, B. C. Shepler, D. Figgen, H. Stoll, J. Phys. Chem. A **110**, 13877 (2006).

[30]M. J. Frisch, G. W. Trucks, H. B. Schlegel, G. E. Scuseria, M. A. Robb, J. R. Cheeseman, G. Scalmani, V. Barone, B. Mennucci, G. A. Petersson, H. Nakatsuji, M. Caricato, X. Li, H. P. Hratchian, A. F. Izmaylov, J. Bloino, G. Zheng, J. L. Sonnenberg, M. Hada, M. Ehara, K. Toyota, R. Fukuda, J. Hasegawa, M. Ishida, T. Nakajima, Y. Honda, O. Kitao, H. Nakai, T. Vreven, J. A. Montgomery, Jr., J. E. Peralta, F. Ogliaro, M. Bearpark, J. J. Heyd, E. Brothers, K. N. Kudin, V. N. Staroverov, R. Kobayashi, J. Normand, K. Raghavachari, A. Rendell, J. C. Burant, S. S. Iyengar, J. Tomasi, M. Cossi, N. Rega, J. M. Millam, M. Klene, J. E. Knox, J. B. Cross, V. Bakken, C. Adamo, J. Jaramillo, R. Gomperts, R. E. Stratmann, O. Yazyev, A. J. Austin, R. Cammi, C. Pomelli, J. W. Ochterski, R. L. Martin, K. Morokuma, V. G. Zakrzewski, G. A. Voth, P. Salvador, J. J. Dannenberg, S. Dapprich, A. D. Daniels, Ö. Farkas, J. B. Foresman, J. V. Ortiz, J. Cioslowski, and D. J. Fox, Gaussian, Inc., Wallingford CT, 2009.

[31]I. Nenner and G. J. Schulz, J. Chem. Phys. **62**, 1747 (1975).

[32]C. Winstead and V. McKoy, Phys. Rev. Lett. **98**, 113201 (2007).

[33]S. W. Staley and J. T. Strnad, J. Chem. Phys. **98**, 116 (1994).

[34]S. A. Pshenichnyuk, N. L. Asfandiarov, and P. D. Burrow, Russ. Chem. Bull. **56**, 1268 (2007).

[35]J. H. Hendricks, J. Chem. Phys. **104**, 7788 (1996).

[36]J. Schiedt, R. Weinkauf, D. M. Neumark, and E. W. Schlag, Chem. Phys. **239**, 511 (1998).

[37]G. A. Gallup and I. I. Fabrikant, Phys. Rev. A **83**, 012706 (2011).

[38]S. Denifl, S. Matejcik, B. Gstir, G. Hanel, M. Probst, P. Scheier, and T. D. Märk, J. Chem. Phys. **118**, 4107 (2003).

[39]X. Li, L. Sanche, and M. D. Sevilla, J. Phys. Chem. B **108**, 5472 (2004).

[40]H. Hotop , M.-W. Ruf, M. Allan, I. I. Fabrikant, Adv. At. Mol. Opt. Phys. **49**, 85 (2003).

[41]P. D. Burrow, A. Modelli, N. S. Chiu, and K. D. Jordan, Chem. Phys. Lett. **82**, 270 (1981).

[42]K. Stricklett, S. Chu, and P. Burrow, Chem. Phys. Lett. **131**, 279 (1986).

[43]W. Domcke, Phys. Rep. **208**, 97 (1991).

[44]P. D. Burrow, G. A. Gallup, A. M. Scheer, S. Denifl, S. Ptasinska, T. Märk, and P. Scheier, J. Chem. Phys. **124**, 124310 (2006).

TABLE I. Exponents of the uncontracted Cartesian Gaussian functions (in atomic units).

Type	Carbon	Nitrogen	Oxygen	Bromine	Iodine
s	12.496280	17.567340	16.058780	6.779740	4.497056
s	2.470286	3.423615	5.920242	1.071059	1.034061
s	0.614028	0.884301	1.034907	0.748707	0.586050
s	0.184028	0.259045	0.316843	0.202254	0.229555
s	0.039982	0.055708	0.065203	0.036220	0.071496
s				0.009055	0.036150
p	5.228869	7.050692	10.141200	4.789276	4.343653
p	1.592058	1.910543	2.783023	1.856547	1.065825
p	0.568612	0.579261	0.841010	0.664700	0.365993
p	0.210326	0.165395	0.232940	0.265909	0.118764
p	0.072250	0.037192	0.052211	0.098552	0.028456
d	0.603592	0.403039	0.756793	0.477153	0.267526
d	0.156753	0.091192	0.180759	0.139024	0.093270

TABLE II. Positions and widths (the latter are given in parenthesis) of the anion states of 5-bromouracil and 5-iodouracil (in units of eV).

5-bromouracil	π_1^*	π_2^*	π_3^*	σ_{CBr}^*
SMC	−0.30	1.50 (0.10)	4.45 (0.46)	0.73 (0.60)
Scaled VOEs	0.03	1.39	3.84	0.72
ET data[8]	< 0	1.3	3.6	~ 1.3
B3LYP/6-311+G(2df,p)[12]	−0.17			
B3LYP/6-31+G(d)[13]	−0.11			
5-iodouracil	π_1^*	π_2^*	π_3^*	σ_{CI}^*
SMC	−0.35	1.54 (0.10)	4.34 (0.45)	−0.10
Scaled VOEs	0.01	1.37	3.65	

TABLE III. Zero-temperature reaction thresholds (in units of eV) for elimination of H (from the N_1 site), X^-, X and HX, where X denotes the halogen atom. The values were computed at the G4(MP2) level, and are presented with and without zero-point vibrational energy correction (the latter in parenthesis).

	H	X^-	X	HX
Uracil	0.85 (1.22)			
5-fluorouracil	0.65 (1.02)	1.71 (1.84)	2.91 (3.08)	−0.02 (0.23)
5-chlorouracil	0.56 (0.92)	0.52 (0.62)	1.85 (1.99)	0.36 (0.65)
5-bromouracil	0.52 (0.89)	0.13 (0.22)	1.25 (1.37)	0.45 (0.73)

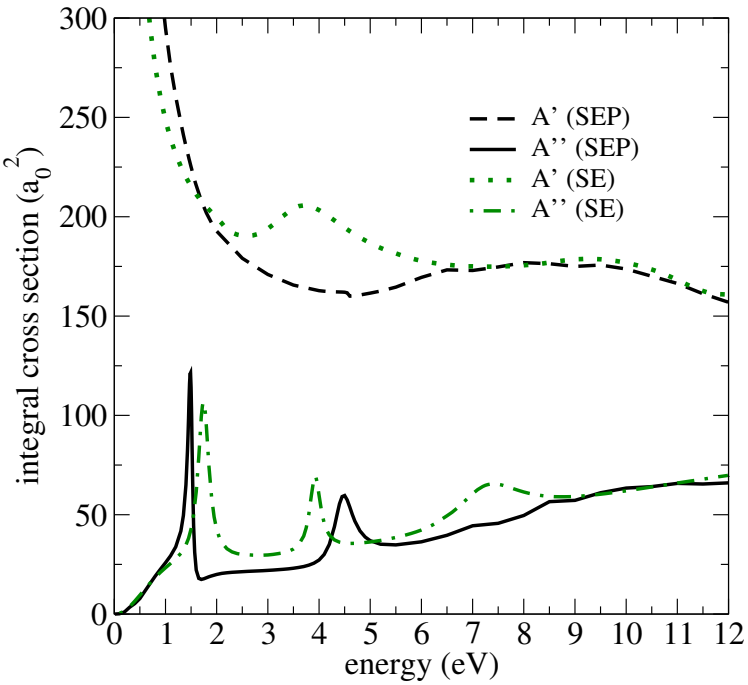

FIG. 1. Integral cross section for the A' and A'' symmetry components of 5-bromouracil, computed at the SE and SEP approximations.

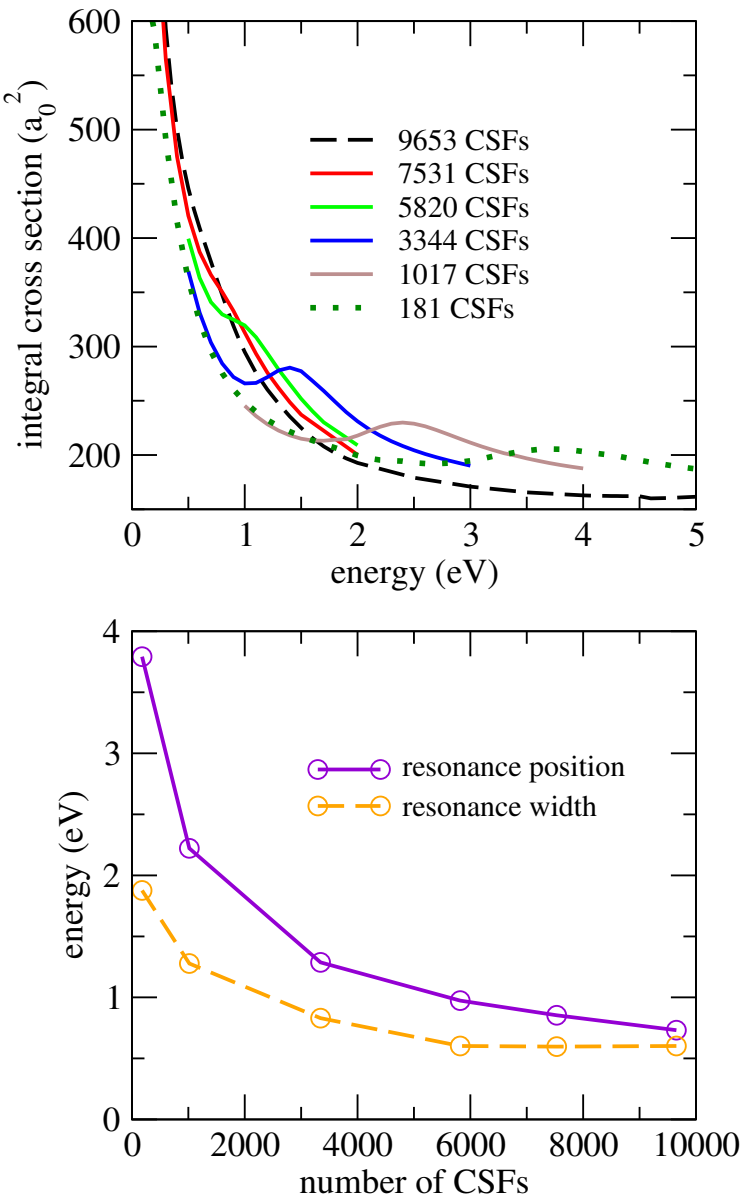

FIG. 2. Upper panel: Integral cross section for the A' symmetry component of 5-bromouracil, calculated in the SE approximation (181 CSFs, also shown in Fig. 1) and by gradually improving the SEP approximation up to the 9653-CSF space (also shown in Fig. 1). As described in the text, the intermediate configuration spaces were obtained from different energy cutoff values (Δ, defined in Sec. II). The corresponding numbers of CSFs employed in each calculation are indicated in the panel. Lower panel: energy position and width of the σ^*_{CBr} resonance obtained from the calculations performed with different polarisation levels, shown in the upper panel, against the dimension of the configuration space (number of CSFs). The lines are guides to the eye.

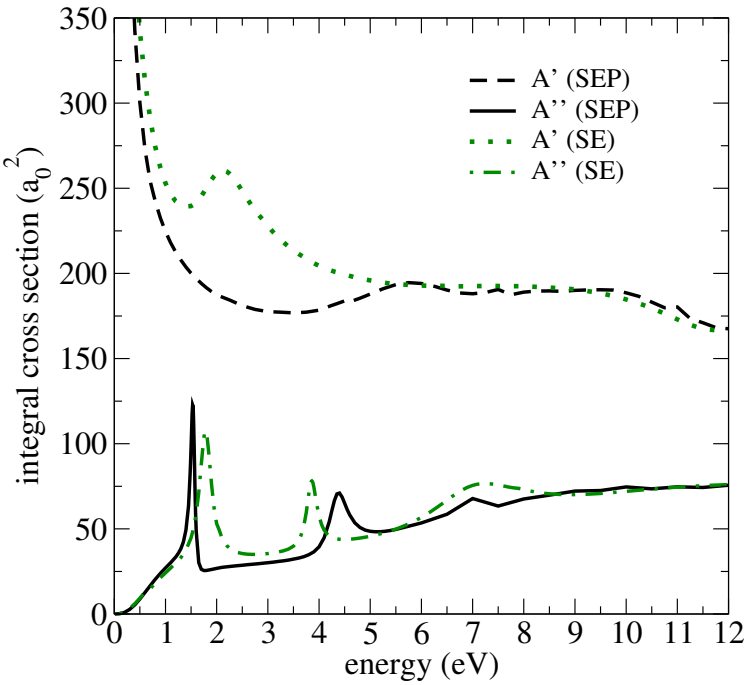

FIG. 3. Integral cross section for the A' and A'' symmetry components of 5-iodouracil, computed at the SE and SEP approximations.

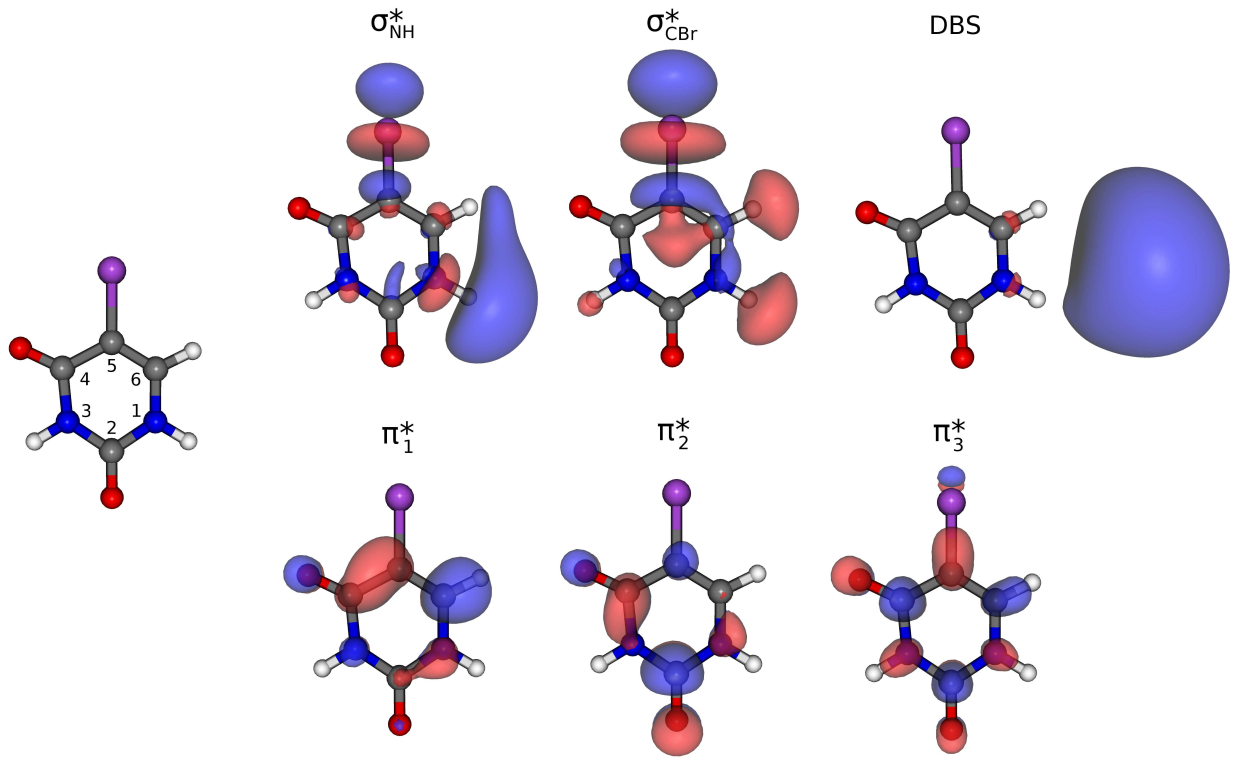

FIG. 4. Structure of 5-bromouracil (left), where the different atoms are indicated by the colours: Br (purple), O (red), N (blue), C (grey) and H (white). The atomic sites on the ring are indicated by the numbers 1 to 6. The low lying π^* (bottom), σ^*_{NH} (upper left) and σ^*_{CBr} (upper middle) virtual orbitals and the singly occupied orbital of the DBS (upper right) are also shown. The plots for the valence and the dipole-bound orbitals correspond to the isovalues of 0.04 and 0.01 a.u., respectively.